Deuteron quadrupole moment and $^3S_1$-$^3D_1$ state properties

Mustafa M. Mustafa
Physics Department, Faculty of Science (Sohag), Assiut University, Sohag, Egypt
(Received 28 April 1992)

Two values for the asymptotic D/S ratio of the deuteron $\eta=0.2701\pm0.00019$ and $\eta=0.02713\pm0.00006$ are obtained using two empirical linear ϵ_1-Q and η-$\gamma^2 Q$ relations we found for standard nonrelativistic potential models. It is shown that fitting the deuteron quadrupole moment Q, the deuteron rms matter radius r_d, and the triplet scattering length a_t simultaneously by a nonrelativistic nucleon-nucleon potential model is a critical task and it has been achieved by the inclusion of a short-range attractive nonlocality in the potential.

PACS number(s): 21.45.+v, 21.30.+y, 13.75.Cs, 21.10.Ft

I. INTRODUCTION

The experimental value of the deuteron quadrupole moment Q, which is one of the most precisely measured deuteron properties (e.g., the results of the last two published measurements of Reid and Vaida [1] $Q^{\exp}=0.2860\pm0.0015$ fm^2 and of Bishop and Cheung [2] $Q^{\exp}=0.2859\pm0.0003$ fm^2 are almost the same), has been used in the literature [3,4] to put constraints on other $^3S_1$-$^3D_1$ state properties. The deuteron quadrupole moment Q is approximately related [5–7] to the scattering mixing parameter ϵ_1 at low energy and to the asymptotic D/S ratio of the deuteron η. The genesis of the relevant approximate formulas is to substitute the asymptotic radial deuteron wave functions

$$u=A_s e^{-\gamma r}\,, \tag{1.1a}$$

$$w=A_s\eta e^{-\gamma r}\left[1+\frac{3}{\gamma r}+\frac{3}{(\gamma r)^2}\right] \tag{1.1b}$$

in the first integral of the formula

$$Q=\frac{1}{\sqrt{50}}\int_0^\infty r^2 uw\,dr-\frac{1}{20}\int_0^\infty r^2 w^2\,dr\,, \tag{1.2}$$

giving Q in impulse approximation, and to neglect the w^2 integral, hence,

$$Q=A_s^2\eta/(\sqrt{8}\gamma^3)\,. \tag{1.3}$$

This is plausible because the D-state probability is relatively small and Q is an "outer" quantity; the r^2 weighting factor in the integrands in (1.2) and the slow fall-off of u and w wave functions as r increases (due to the smallness of the binding energy γ^2) make the main contribution to Q come from outside the range of force.

Blatt and Weisskopf [5] used in Eq. (1.3) $A_s^2=2\gamma$ given by $\int_0^\infty u^2 dr=1$ and obtained

$$\epsilon_1=\sqrt{2}Qk^2\,, \tag{1.4}$$

where k^2 is a positive low energy. Biedenharn and Blatt [6] used in Eq. (1.3) $A_s^2=2\gamma/\{(1-\gamma\rho)(1+\eta^2)\}$, given by the effective range but with the assumptions $\eta^2\ll 1$ and $\rho\approx r_t$

$$\epsilon_1=(1-\gamma r_t)\sqrt{2}Qk^2\,. \tag{1.5}$$

The factor ( ) is written ( )^2 in the paper of Biedenharn and Blatt [6]. Bulter and Sprung [7] have shown that the second integral in Eq. (1.2) is about $\frac{1}{16}$ of the first and they modified relation (1.5) by incorporating the multiplication factor $\frac{16}{15}$ on the right-hand side.

Two different cases will be considered in the following discussion of the relations connecting ϵ_1, Q, and k^2. The first case is to consider one single potential model and to see a possible correlation between its value of Q and its values of ϵ_1 which change smoothly and continuously with the scattering energies. The second case is to consider a large number of potential models and a certain value of scattering energy k^2 and then to calculate for each ith potential its model values $Q^{(i)}$ and $\epsilon_1^{(i)}$.

In the first case, when considering a single potential model, poor results are obtained for the value of Q by using [8]

$$Q=\frac{1}{\sqrt{2}}\frac{d\epsilon_1}{dk^2}\bigg|_{k^2=0}$$

implied by Eq. (1.4), and [4,9]

$$Q=\{\sqrt{2}(1-\gamma r_t)\}^{-1}\frac{d\epsilon_1}{dk^2}\bigg|_{k^2=0}$$

implied by Eq. (1.5). It has been shown [10] that in this case of a given single potential model, the smooth variation of ϵ_1 with energy is not a linear relation even at very low energies. In the second case, when considering a large number of standard nonrelativistic nucleon-nucleon N-N potential models at a fixed very low energy in the laboratory scattering range 0–1 MeV, the points $(Q^{(i)},\epsilon_1^{(i)})$ representing the potential models lie on a typical straight line which does not pass through the experimental points $(Q^{\exp},\epsilon_1^{\exp})$ reported within this range of energy [10]. For such empirical ϵ_1-Q lines (of case 2) drawn at fixed values of low scattering energy k^2 (see Fig. 1), and using the "eigen" scattering mixing parameter ϵ_1 of the Biedenharn and Blatt parametrization [6], it is

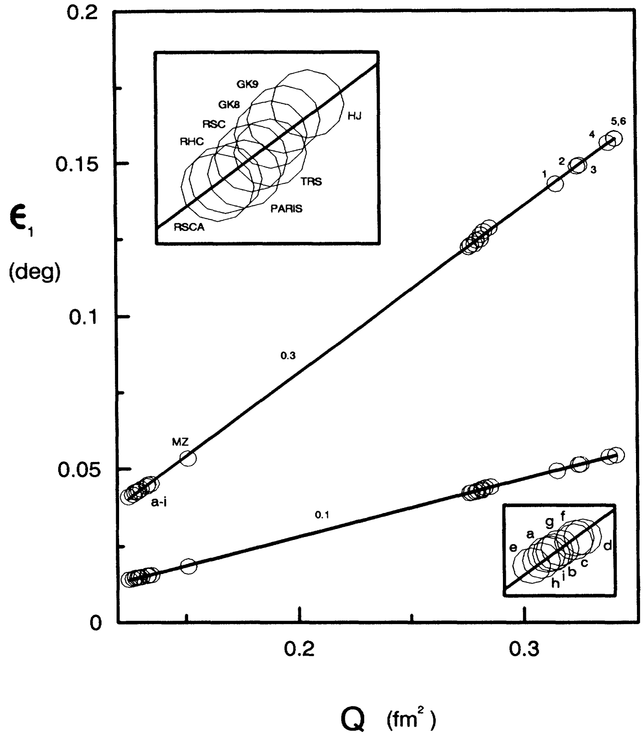

FIG. 1. The empirical ϵ_1-Q lines for the scattering energies $E_{\text{c.m.}}=0.1$ and 0.3 MeV. The middle (lower) part of the upper line is magnified in the upper (lower) inner frame. The potentials are referred to by the names given in Table II. The ϵ_1 is the "eigen" mixing parameter of the Biedenharn and Blatt parametrization [6].

shown in this paper (Sec. II) that

$$\left.\frac{\epsilon_1}{(k^2Q)}\right|_{k^2=0}\approx\sqrt{2}$$

and that the empirical ϵ_1-Q lines can be used to determine a new value of η (Sec. III). Another value of η is also obtained from the empirical linear η-$Q\gamma^2$ relation between η and $\gamma^2 Q$ of potential models implied by (1.4).

Klarsfeld *et al.* [11] found that the relation between the triplet scattering length a_t and the deuteron root-mean-square (rms) radius r_d of standard nonrelativistic potential models is a typical straight line which does not pass through the experimental point $a_t=5.419\pm0.007$ fm [12] and $r_d=1.953\pm0.003$ fm [11]. Mustafa and Hassan [13] and van Dijk [14] have shown that short-range nonlocality can change r_d without changing a_t. Kermode *et al.* [15,16], Mustafa and Kermode [17], and Mustafa *et al.* [18] fitted the experimental values of a_t and r_d simultaneously by potential models incorporating short-range attractive nonlocal components. These potentials [15,18], which fit a_t and r_d simultaneously, do not also fit the experimental value of the deuteron quadrupole moment Q. It is shown in Sec. IV, and by using the unitary transformations, that fitting Q, r_d, and a_t by a potential model is a "critical" task. This could be achieved (Sec. V) by the inclusion of an attractive short-range nonlocality in the potential model.

Bhaduri *et al.* [19] and Sprung *et al.* [20] have looked into the relationships between r_d and the asymptotic quantities a_t and r_t which are determined by the low-energy dependence of the $^3S_1$ phase shifts. This is different from the present analysis involving the deuteron quadrupole moment Q, since Q is intimately related to both the mixing parameter ϵ_1 at low energies (Sec. II) and to the noncentral forces of the nucleon-nucleon interaction. Also, Q is not a pure asymptotic quantity (e.g., phase equivalent potentials can have different values of Q [8,21,22]) and it is more directly observable than r_t. The present analysis emphasizes, in particular, the influence of the tensor force on the value of r_d.

II. ϵ_1 AT LOW ENERGIES AND THE APPROXIMATE RELATION OF BLATT AND WEISSKOPF

The N-N potential models being used to draw the empirical ϵ_1-Q lines are the standard potential models (with reasonable values of Q and ϵ_1 at low energy range): e.g., the potential models of Lacombe *et al.* [23], de Tourreil *et al.* [24], Reid [25], Hamada and Johnston [26], and Glendenning and Kramer [27], in addition to the local potentials of Mustafa and Zahran [28] and Mustafa [29] which have extremely low values of ϵ_1 and Q, and, the local potentials referred to as 1–6 of Table I, which have extremely high values of ϵ_1 and Q_1.

The potentials 1–6 fit the deuteron binding energy [30]

$$E_b=-2.224\,575\pm0.000\,009\ \text{MeV}$$

and the scattering parameters of Arndt *et al.* [31] in the laboratory scattering energy range 0–300 MeV with $\chi^2/\text{datum}\approx0.02$. They reproduce well, in particular, the relatively "large" experimental values of ϵ_1 at low energies even better than the local potentials $r1$–$r7$ of Ref. [10]. The functional form of the local potentials 1–6 is similar to that of the Reid hard-core (RHC) potential [25]. It consists of central (C), spin-orbit (LS), and tensor (T) parts:

$$V=V_C+V_{LS}\mathbf{L}\cdot\mathbf{S}+S_{12}V_T \tag{2.1}$$

where

$$rV_i(r)=\sum_{n=1}^{6}A_i(n)e^{-n\mu r}\ ,\quad i=C,LS\ , \tag{2.2a}$$

$$rV_T=A_T(1)(Y_1-Y_6)+\sum_{n=2}^{n=6}A_T(n)e^{-n\mu r}\ , \tag{2.2b}$$

$$Y_n=n^2[1+3/n\mu r+3/(n\mu r)^2]e^{-n\mu r}\ . \tag{2.2c}$$

$A_i(1)$ is determined by the one pion exchange potential, i.e.,

$$A_C(1)=A_T(1)=-14.947\,14\ \text{MeV fm}$$

and $A_{LS}(1)=0.0$ and $\mu=0.7\ \text{fm}^{-1}$.

"Experimental" values ϵ_1^{exp} of the scattering mixing parameter ϵ_1 in the center-of-mass scattering energy range 0–0.55 MeV have been extracted from 36 empirical ϵ_1-Q lines; they are the values of ϵ_1 which correspond to the experimental value $Q^{\text{exp}}=0.2859\pm0.0003\ \text{fm}^{-2}$ [2] of the deuteron quadrupole moment. Two such lines are shown in Fig. 1. The very-low-energy dependence of the "experimental" scattering mixing parameter $\epsilon_1^{\exp}$ is compared to those of some potential models and of the Mathelitsch and VerWest empirical formula [32] $\epsilon_1 = 0.347k^2(1+5.5k^2)^{-1}$ in Fig. 2. The two graphs of $\epsilon_1^{\exp}$ and ϵ_1 of the Glendenning and Kramer GK9 potential [27] are indistinguishable by the scale used. The value of the scattering mixing parameter ϵ_1 of Arndt

TABLE I. The values of the free parameters and the hard-core radii of the local potentials.

Potential	r_C	n	$A_C(n)$	$A_{LS}(n)$	$A_T(n)$
1	0.35	2	−1.965 898 9 (3)	2.918 453 6 (2)	−7.292 287 3 (2)
		3	3.190 564 9 (4)	−3.489 898 6 (3)	9.752 595 7 (3)
		4	−1.656 421 0 (5)	2.206 868 8 (4)	−4.116 681 2 (4)
		5	3.381 626 2 (5)	−6.262 238 2 (4)	6.257 800 5 (4)
		6	−2.390 524 6 (5)	6.343 780 0 (4)	−2.402 322 4 (4)
2	0.4	2	−2.148 337 3 (3)	3.555 918 2 (2)	−8.010 167 4 (2)
		3	3.675 488 6 (4)	−3.793 774 5 (3)	1.046 434 1 (4)
		4	−2.002 526 1 (5)	2.246 270 5 (4)	−4.343 785 4 (4)
		5	4.313 632 1 (5)	−6.368 558 2 (4)	6.261 227 6 (4)
		6	−3.242 717 3 (5)	6.647 793 0 (4)	−1.779 767 7 (4)
3	0.45	2	−2.193 696 4 (3)	4.677 039 3 (2)	−8.273 914 5 (2)
		3	3.840 562 2 (4)	−6.274 254 2 (3)	1.086 963 7 (4)
		4	−2.144 960 1 (5)	3.819 907 8 (4)	−4.605 263 8 (4)
		5	4.696 927 1 (5)	−9.583 563 9 (4)	7.373 893 7 (4)
		6	−3.502 350 4 (5)	8.004 787 2 (4)	−3.719 216 1 (4)
4	0.5	2	−1.859 988 8 (3)	6.318 604 3 (2)	−9.847 016 6 (2)
		3	3.305 842 4 (4)	−8.713 795 9 (3)	1.362 483 4 (4)
		4	−1.900 311 3 (5)	5.704 043 1 (4)	−6.412 288 7 (4)
		5	4.342 904 7 (5)	−1.663 457 0 (5)	1.196 529 0 (5)
		6	−3.416 000 1 (5)	1.714 972 2 (5)	−7.445 572 4 (4)
5	0.548 33	2	−2.336 855 8 (3)	6.552 651 4 (2)	−1.064 920 6 (3)
		3	4.338 559 7 (4)	−8.728 817 3 (3)	1.520 646 8 (4)
		4	−2.567 949 0 (5)	5.198 942 1 (4)	−7.429 276 3 (4)
		5	6.015 317 4 (5)	−1.300 832 6 (5)	1.447 205 6 (5)
		6	−4.846 072 9 (5)	1.111 626 6 (5)	−9.510 766 8 (4)
6	0.55	2	−2.364 565 4 (3)	5.965 594 8 (2)	−1.070 279 7 (3)
		3	4.444 294 9 (4)	−7.301 314 7 (3)	1.527 231 4 (4)
		4	−2.664 398 7 (5)	4.171 171 0 (4)	−7.419 410 5 (4)
		5	6.309 848 1 (5)	−1.029 143 2 (5)	1.432 290 4 (5)
		6	−5.123 751 6 (5)	8.805 459 9 (4)	−9.305 780 6 (4)
a	0.548 33	2	−1.581 512 2 (3)	5.322 331 1 (2)	−8.137 058 8 (2)
		3	3.009 415 0 (4)	−7.394 491 2 (3)	1.239 230 3 (4)
		4	−1.802 580 8 (5)	4.478 642 7 (4)	−6.352 273 8 (4)
		5	4.248 162 4 (5)	−1.144 741 7 (5)	1.298 215 8 (5)
		6	−3.455 271 1 (5)	1.001 653 9 (5)	−8.949 689 0 (4)
*L*1	0.548 33	2	−4.275 790 0 (2)	5.251 529 6 (2)	−5.955 005 9 (2)
		3	1.146 640 2 (4)	−7.227 502 3 (3)	9.567 210 6 (3)
		4	−8.090 928 9 (4)	4.086 843 8 (4)	−4.953 419 0 (4)
		5	2.102 828 3 (5)	−1.027 498 3 (5)	1.019 028 6 (5)
		6	−1.858 656 4 (5)	9.102 665 1 (4)	−7.035 361 2 (4)
*L*2	0.548 33	2	−2.835 829 5 (2)	6.748 478 7 (2)	−6.002 338 0 (2)
		3	8.720 842 7 (3)	−1.045 810 2 (4)	9.323 583 9 (3)
		4	−6.547 943 7 (4)	6.261 212 0 (4)	−4.606 367 8 (4)
		5	1.780 060 9 (5)	−1.586 168 3 (5)	8.928 228 1 (4)
		6	−1.636 814 0 (5)	1.379 787 4 (5)	−5.731 217 5 (4)

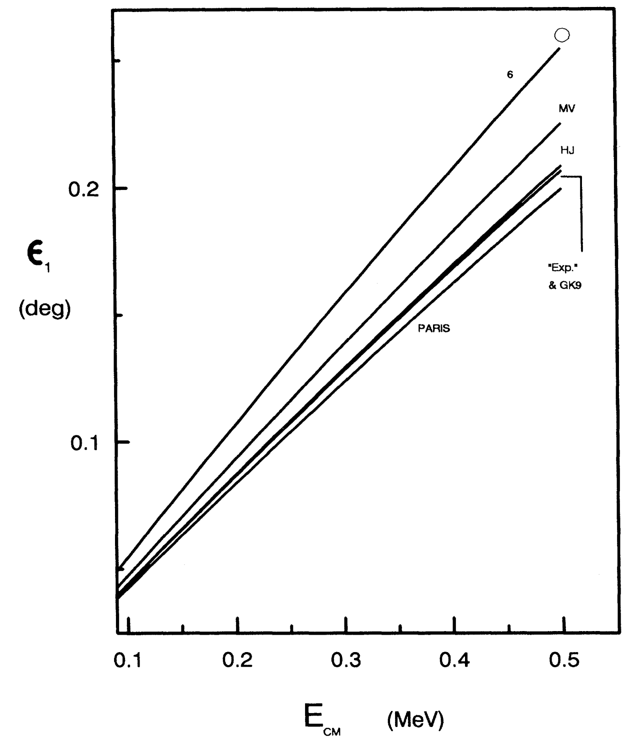

FIG. 2. The low-energy dependence of the "experimental" mixing parameter ϵ_1 is compared to the corresponding energy dependences of some potential models and of the empirical formula of Mathelitsch and VerWest (MW) [32]. The experimental point (circle) is of Arndt *et al.* [31]. The references to the potentials are the same as in Fig. 1.

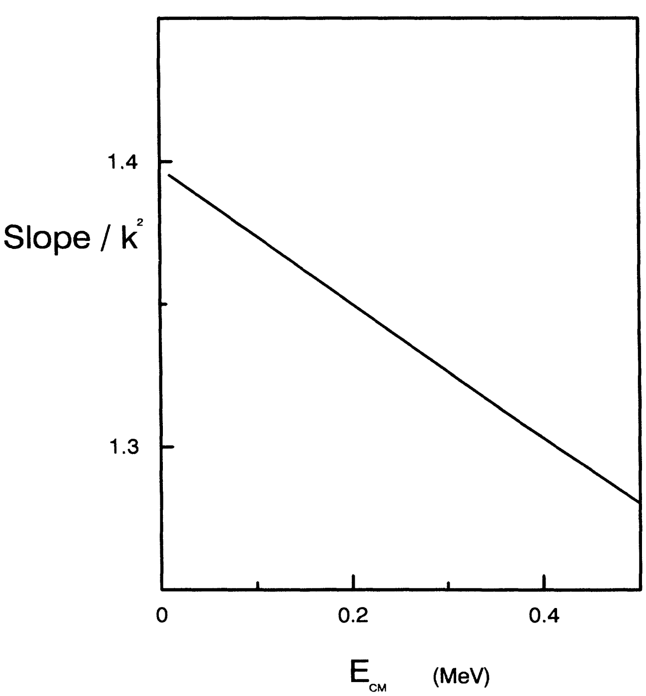

FIG. 3. The variation versus the center-of-mass c.m. scattering energy $E_{\mathrm{c.m.}}$ of the quotient (slope/k^2), given by dividing the slope of an empirical ϵ_1-Q line by k^2 of that line.

et al. [31] at $E_{\mathrm{c.m.}}=0.5$ MeV, represented by a circle in Fig. 2, is given in the "eigen" parametrization of Biedenharn and Blatt [6] [by using both the published values of the scattering parameters $\delta(^3S_1)$, $\delta(^3D_1)$ and ϵ_1 given in the "bar" parametrization of Stapp *et al.* [33] and the relations [34] between the "eigen" and the "bar" parametrization]. The high quality fitting of ϵ_1 of Arndt *et al.* [31] with the potentials 1-6 of Table I may be seen from Fig. 2 (only the potential 6 is drawn).

The slope of an ϵ_1-Q line divided by k^2 would be 1.398 upon extrapolation to zero scattering energy (Fig. 3), which is about 1% smaller than $\sqrt{2}$, in agreement with Eq. (1.4).

III. VALUES OF η CONSISTENT WITH Q^{exp}

A. η from the very-low-energy dependence of ϵ_1

The very-low-energy dependence $\epsilon_1=\epsilon_1(k^2)$ of the experimental scattering mixing parameter $\epsilon_1^{\mathrm{exp}}$ is extrapolated to the deuteron bound state to obtain the deuteron asymptotic D/S ratio η, where

$$\eta=-\epsilon_1(-\gamma^2)\ . \tag{3.1}$$

The reliability of this method is first checked by using model values of ϵ_1. The very-low-energy dependence of ϵ_1 of a given potential model is fitted by a polynomial of fifth order in k^2 (36 data pieces, in the center-of-mass scattering energy range 0–0.55 MeV), and as shown in Table II the substitution $k^2=-\gamma^2$ gave a value $\bar{\eta}$ for the asymptotic ratio which is almost the same as that obtained from the deuteron waves η. The experimental value

$$\eta=0.027\,009\pm0.000\,007 \tag{3.2a}$$

is obtained for η by applying the same procedure to the experimental mixing parameter $\epsilon_1^{\mathrm{exp}}$ of Fig. 2, and using the experimental value of the deuteron binding energy $E_b=2.224\,575\pm0.000\,009$ MeV [30], where, $\gamma^2=E_b/41.471\,397\ \mathrm{fm}^{-2}$. A similar value

$$\eta=0.027\,003\pm0.000\,007 \tag{3.2b}$$

is obtained by using in Eq. (3.1) $\tan\epsilon_1$ instead of ϵ_1. Practically; $\epsilon_1\approx\tan\epsilon_1$ within this very-low-energy range. The corresponding results for the potential models are also listed in Table II. Although the small standard errors in Eqs. (3.2) are smaller than the values of $\eta-\bar{\eta}$, it is more convenient to choose for the standard error the largest model value obtained for $\eta-\bar{\eta}$. Hence,

$$\eta=0.027\,01\pm0.000\,19 \tag{3.3}$$

represents the result of this method.

B. η from the η-γ^2Q empirical line

The relation between η and γ^2Q of standard nonrelativistic potential models—as implied by the approximate relation (1.4) of Blatt and Weisskopf [5]—is a typical line as shown in Fig. 4. The potential models used in Fig. 4 are the same as those used in Fig. 1, plus the potentials of

TABLE II. The difference $\eta-\bar{\eta}$ between the two values obtained for the asymptotic D/S ratio η (using the deuteron waves) and $\bar{\eta}$ (using the low energy dependence of ϵ_1). The potentials are ordered in the table by their quality of fitting $\epsilon_1^{\mathrm{exp}}$ of Fig. 2. The lower values are for the case of using $\tan\epsilon_1$ instead of ϵ_1 in Eq. (3.1). The standard errors are only listed for the experimental data; they are smaller than the largest value of $|\eta-\bar{\eta}|$ in all cases.

Pot.	Ref.	η	$\bar{\eta}$	$\eta-\bar{\eta}$
GK9	[27]	0.026 709	0.026 614	0.000 095
			0.026 630	0.000 079
HJ	[26]	0.026 485	0.026 369	0.000 116
			0.026 336	0.000 149
GK8	[27]	0.026 592	0.026 425	0.000 167
			0.026 406	0.000 186
TRS	[24]	0.026 222	0.026 226	−0.000 004
			0.026 230	0.000 007
RSC	[25]	0.026 226	0.026 106	−0.000 120
			0.026 121	−0.000 105
Paris	[23]	0.026 080	0.026 101	0.000 021
			0.026 121	0.000 042
RHC	[25]	0.025 902	0.025 825	0.000 077
			0.025 813	0.000 089
RSCA	[25]	0.025 958	0.025 846	−0.000 112
			0.025 820	−0.000 138
1		0.030 151	0.030 188	0.000 036
			0.030 187	0.000 036
2		0.031 176	0.031 208	−0.000 023
			0.031 219	−0.000 044
3		0.031 308	0.031 175	0.000 133
			0.031 208	0.000 100
4		0.032 766	0.032 866	−0.000 100
			0.032 830	−0.000 064
6		0.033 085	0.033 107	−0.000 022
			0.033 102	−0.000 017
5		0.033 095	0.033 094	−0.000 001
			0.033 082	0.000 012
MZ	[28]	0.013 353	0.013 216	0.000 137
			0.013 224	0.000 129
d	[29]	0.011 702	0.011 592	0.000 110
			0.011 593	0.000 109
f	[29]	0.011 550	0.011 441	0.000 109
			0.011 438	0.000 112
c	[29]	0.011 538	0.011 415	0.000 123
			0.011 419	0.000 119
g	[29]	0.011 260	0.011 144	0.000 116
			0.011 150	0.000 110
b	[29]	0.011 161	0.011 050	0.000 111
			0.011 048	0.000 113
i	[29]	0.011 090	0.010 962	0.000 128
			0.010 948	0.000 142
a	[29]	0.010 979	0.010 892	0.000 087
			0.010 887	0.000 092
h	[29]	0.010 904	0.010 789	0.000 115
			0.010 781	0.000 123
e	[29]	0.010 702	0.010 575	0.000 128
			0.010 568	0.000 134
Exp. (this work)			0.027 009±0.000 007	
			0.027 003±0.000 007	

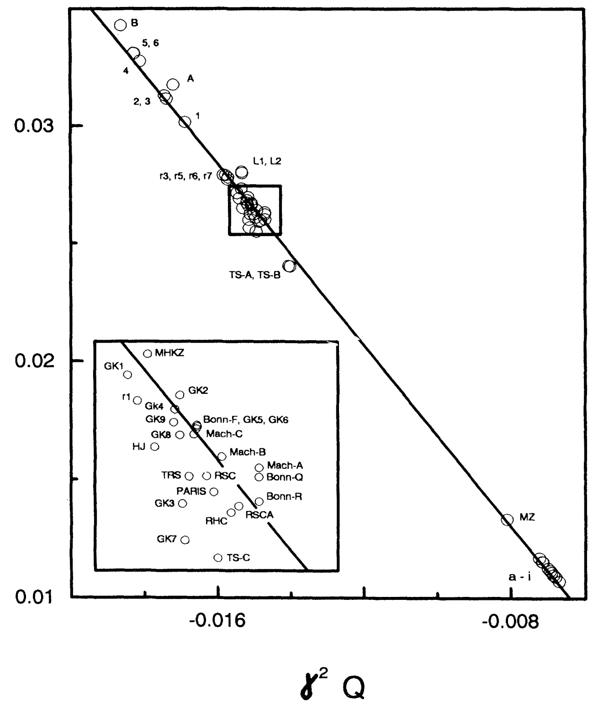

FIG. 4. The variation of the deuteron asymptotic D/S ratio η versus $\gamma^2 Q$ of deuteron potential models. The potentials used are the same as in Fig. 1 plus $r1$–$r7$ of Mustafa *et al.* [10], MHKZ of Mustafa *et al.* [18], "Bonn" of Machleidt *et al.* [35], "Mach" of Machleidt [36], A and B of Mustafa [37], TS of de Tourreil and Sprung [38], and the potentials $L1$ and $L2$ of Table I. The middle part of the graph is magnified in the inner frame.

Machleidt *et al.* [35], Machleidt [36], Mustafa *et al.* [10,18], Mustafa [37], de Tourreil *et al.* [24], de Tourreil and Sprung [38], and the local potentials $L1$ and $L2$ of Table I. The experimental value

$$\eta = 0.027\,13 \pm 0.000\,06 \tag{3.4}$$

is obtained as the value of η corresponding to the experimental values of both the deuteron quadrupole moment $Q^{\exp} = 0.2859 \pm 0.0003\ \text{fm}^{-2}$ [2] and the deuteron binding energy $E_b = 2.224\,575 \pm 0.000\,009$ MeV [30].

As revealed by the relations (3.3) and (3.4), the two independent methods of the Secs. III A and III B gave very similar values for η, which is evidence that the experimental data favor these two determinations.

The two values of η of Eqs. (3.3) and (3.4) are also in agreement, within the quoted errors, with the most recent published values $\eta = 0.027\,12 \pm 0.000\,22$ of Stokes *et al.* [39] and $\eta = 0.0273 \pm 0.0005$ of Borbély *et al.* [40].

IV. CRITICALITY OF FITTING Q, r_d, AND a_t SIMULTANEOUSLY BY A POTENTIAL MODEL

Unitary transformations of the following form used by Kermode *et al.* [8] are used to find nonlocal potentials fitting simultaneously Q, r_d, and a_t:

$$Z = \begin{bmatrix} Z_u & 0 \\ 0 & Z_w \end{bmatrix}$$

where

$$Z_u = Z_w = 1 - 2g(s)g(s') ,$$

$$g(s) = Cs(1-\beta s)e^{-\alpha s} ,$$

$$s = r - r_C ,$$

$$C = [4\alpha^5/(\alpha^2 - 3\alpha\beta + 3\beta^2)]^{1/2} .$$

r_C is the hard-core radius and C is a normalizing constant such that $\langle g|g \rangle = 1$.

The unitary transformations are applied to the radial deuteron wave functions u and w of three local potentials which fit the experimental value $a_t = 5.149 \pm 0.007$ fm of Klarsfeld *et al.* [12]. These three potentials are the potential referred to as a in Table I, the potential C of Machleidt [36], and the Paris potential of Lacombe *et al.* [23]. The potential a fits well the experimental scattering parameters of Arndt *et al.* [31] in the laboratory scattering energy range 0–300 MeV. Its functional form is defined by the relations (2.1) and (2.2).

Pairs of values of α and β producing transformed waves with correct r_d or correct Q are represented by points (α,β) which lie on typical smooth lines in the α-β diagram of Fig. 5. A point of intersection between the line of correct r_d and the line of correct Q would correspond to a nonlocal potential having the correct experimental values of Q, r_d, and a_t. The lack of such intersection points [see Figs. 5(a)–5(c)] reveals the difficulty of fitting Q, r_d, and a_t by deuteron potential models; it may point out the existence of a possible correlation between these quantities. The Reid hard-core potential [25] having $a_t = 5.397$ fm, which disagrees with experiment, has the interesting point $(\alpha,\beta) = (2.325, 1.103)$ corresponding to a nonlocal potential fitting r_d and Q but not a_t [see Figs. 5(d) and 6(a)].

The local potentials $L1$ and $L2$ of Table I fit both Q and r_d, but not a_t. The shapes of the D-state wave functions of these potentials [Fig. 6(b)] are expected for nonlocal potentials, but we emphasize that these are the result for *local* potentials.

It is interesting to note both the signs and the shapes of the transformed radial u and w wave functions produced by using points (α,β) of the graphs of Fig. 5(a) [Fig. 5(a) is taken as an example]. For a given value of α in the

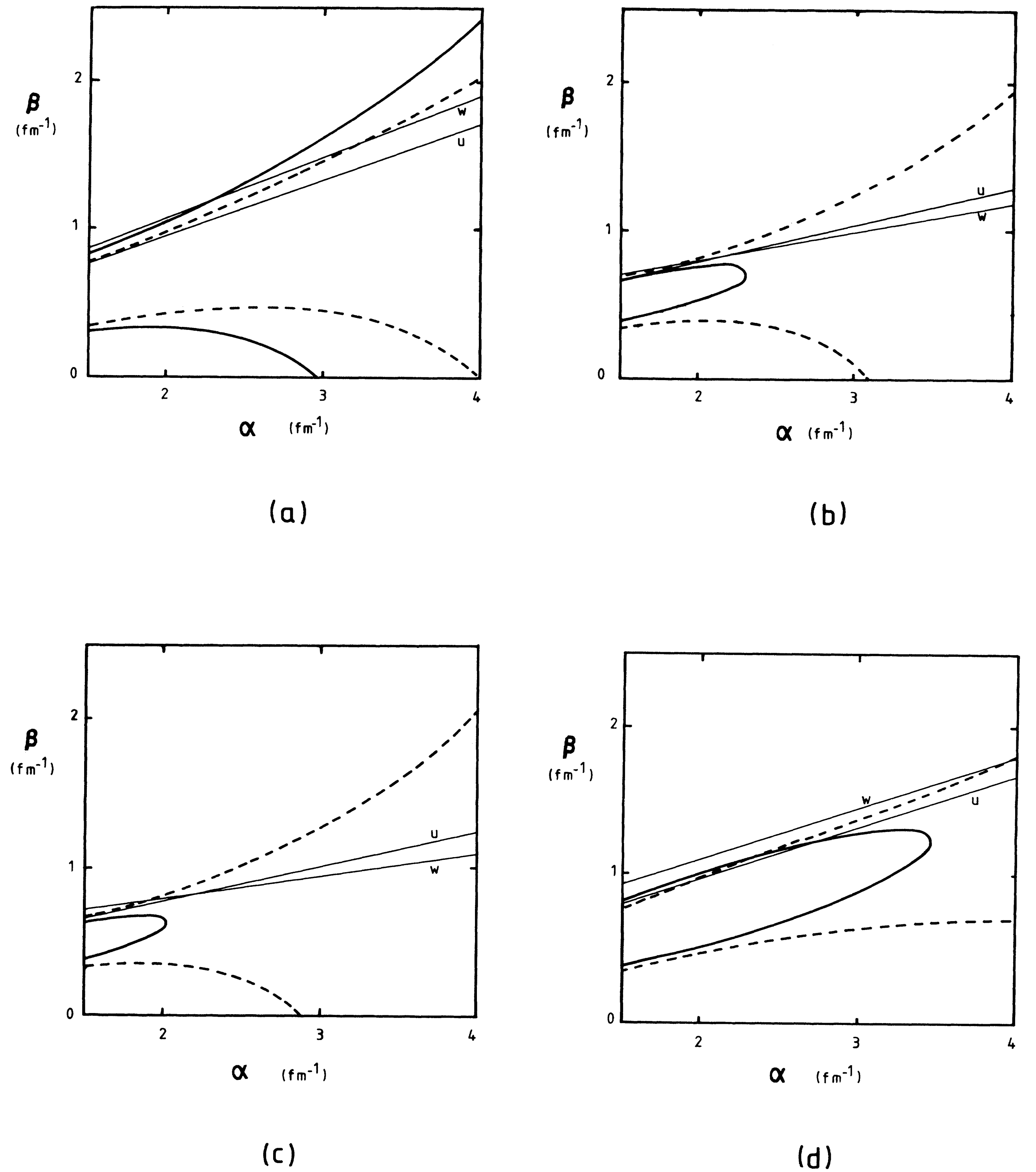

FIG. 5. Using pairs of values of the two parameters α and β of the unitary transformations represented by points (α,β) on the solid thick lines (dashed lines) will produce transformed waves having the correct $Q(r_d)$. The local reference potentials are (a) the potential a of Table I, (b) the potential C of Machleidt [36], (c) the Paris potential [23], and (d) the Reid hard-core (RHC) potential [25]. The transformed and the untransformed u (w) wave functions will be the same if a point (α,β) on the straight thin solid line labeled u (w) is used.

TABLE III. The values of the free parameters of the nonlocal potential which has the correct Q, r_d, and a_t. $\lambda = -325\ \text{fm}^{-3}$ and $r_C = 0.548\,33$ fm.

n	$A_C(n)$	$A_{LS}(n)$	$A_T(n)$
2	$-2.134\,451\,8$ (3)	$2.706\,493\,7$ (2)	$-5.203\,594\,6$ (2)
3	$4.351\,722\,2$ (4)	$-5.429\,413\,6$ (3)	$7.063\,765\,1$ (3)
4	$-2.790\,110\,8$ (5)	$4.993\,148\,5$ (4)	$-2.678\,949\,5$ (4)
5	$7.878\,579\,9$ (5)	$-1.588\,838\,3$ (5)	$3.429\,146\,9$ (4)
6	$-7.379\,260\,5$ (5)	$1.506\,265\,9$ (5)	$-9.554\,318\,2$ (3)

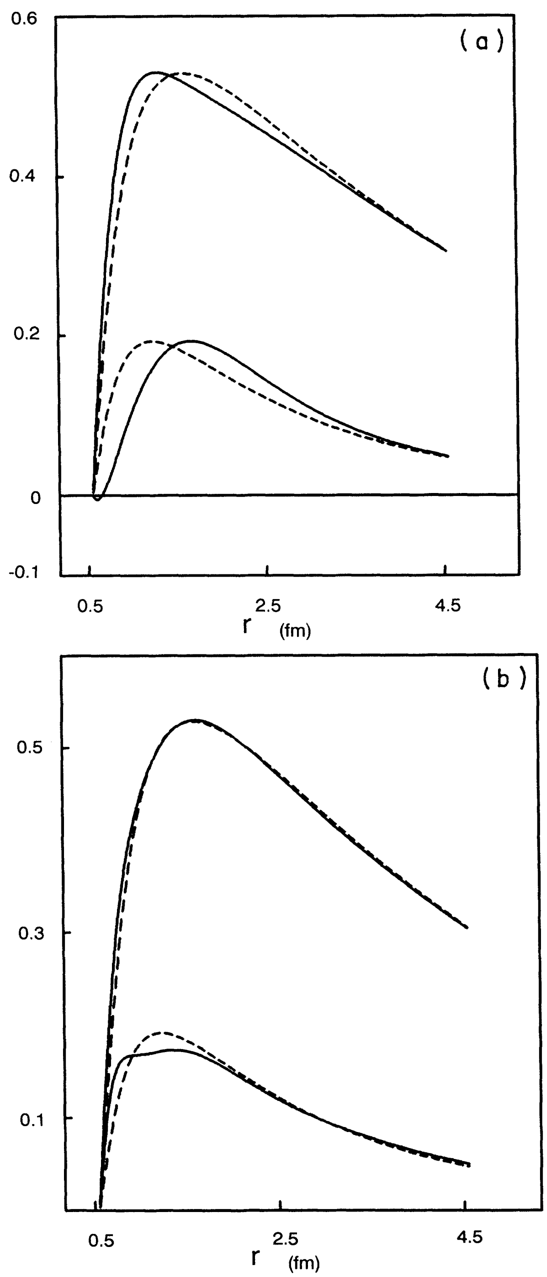

FIG. 6. The radial deuteron wave functions having the correct Q and r_d (solid lines), (a) determined by the intersection point $\alpha = 2.325\ \text{fm}^{-1}$ and $\beta = 1.103\ \text{fm}^{-1}$ of Fig. 5(d), and (b) of the local potential $L1$ of Table I, are compared to the Reid hard-core potential [25] (dashed lines). The upper (lower) curves are the u (w) wave functions.

range $\alpha \geq 1.5\ \text{fm}^{-1}$, two pairs of values of β may be found, the first [second] pair corresponds to the correct r_d [Q]. The transformed wave functions are positive [negative] at small radii if the larger [smaller] value of β is used, which means using a point on the upper [lower] graph, as shown in Fig. 7(a) [7(b)]. The transformed waves using points (α,β) of the upper graphs have short-range structures [Figs. 7(a) and 7(c)] similar to those of the potentials [15–18] which incorporate short-range attractive nonlocality. The "complexity" of these structures [Fig. 7(c)] increases with "increasing" nonlocality (i.e., by using relatively large values for α and β).

V. A POTENTIAL MODEL WITH CORRECT Q, r_d, AND a_t

It was possible to fit Q, r_d, and a_t simultaneously by a nonlocal potential model incorporating short-range attractive nonlocality with equal strengths in both S and D states (see Table III). This nonlocal potential consists of a local part $V^{(L)}$ plus a nonlocal attractive separable part $V^{(N)}$:

$$V = V^{(L)} + V^{(N)} . \tag{5.1}$$

The functional forms chosen for the local part $V^{(L)}$ are defined by the relations (2.1) and (2.2). The coupled radial Schrödinger equations in this case have the following form:

TABLE IV. Properties of the nonlocal potential of Table III.

Binding energy E_b	2.2242 MeV
Quadrupole moment Q	0.2862 fm^2
D-state probability p_D	6.544%
Asymptotic S-state amplitude A_S	0.8898 fm$^{-1/2}$
Asymptotic D-state amplitude A_D	0.0255 fm$^{-1/2}$
The asymptotic ratio $\eta = A_D/A_S$	0.0287
rms radius r_d	1.953 fm
D_2 parameter	0.5317 fm^2
Scattering length a_t	5.418 fm
Effective range r_t	1.724 fm
Shape parameter P	0.039

$$\left[\frac{d^2}{dr^2}-V_C-\gamma^2\right]u(r)-2\sqrt{2}V_T w(r) -\lambda f(r)\int_{r_C}^{\infty} f(r')u(r')dr'=0 , \quad (5.2a)$$

$$\left[\frac{dr^2}{dr^2}-\frac{6}{r^2}-V_C+3V_{LS}+2V_T-\gamma^2\right]w(r)-2\sqrt{2}V_T u(r) -\lambda f(r)\int_{r_C}^{\infty} f(r')w(r')dr'=0 , \quad (5.2b)$$

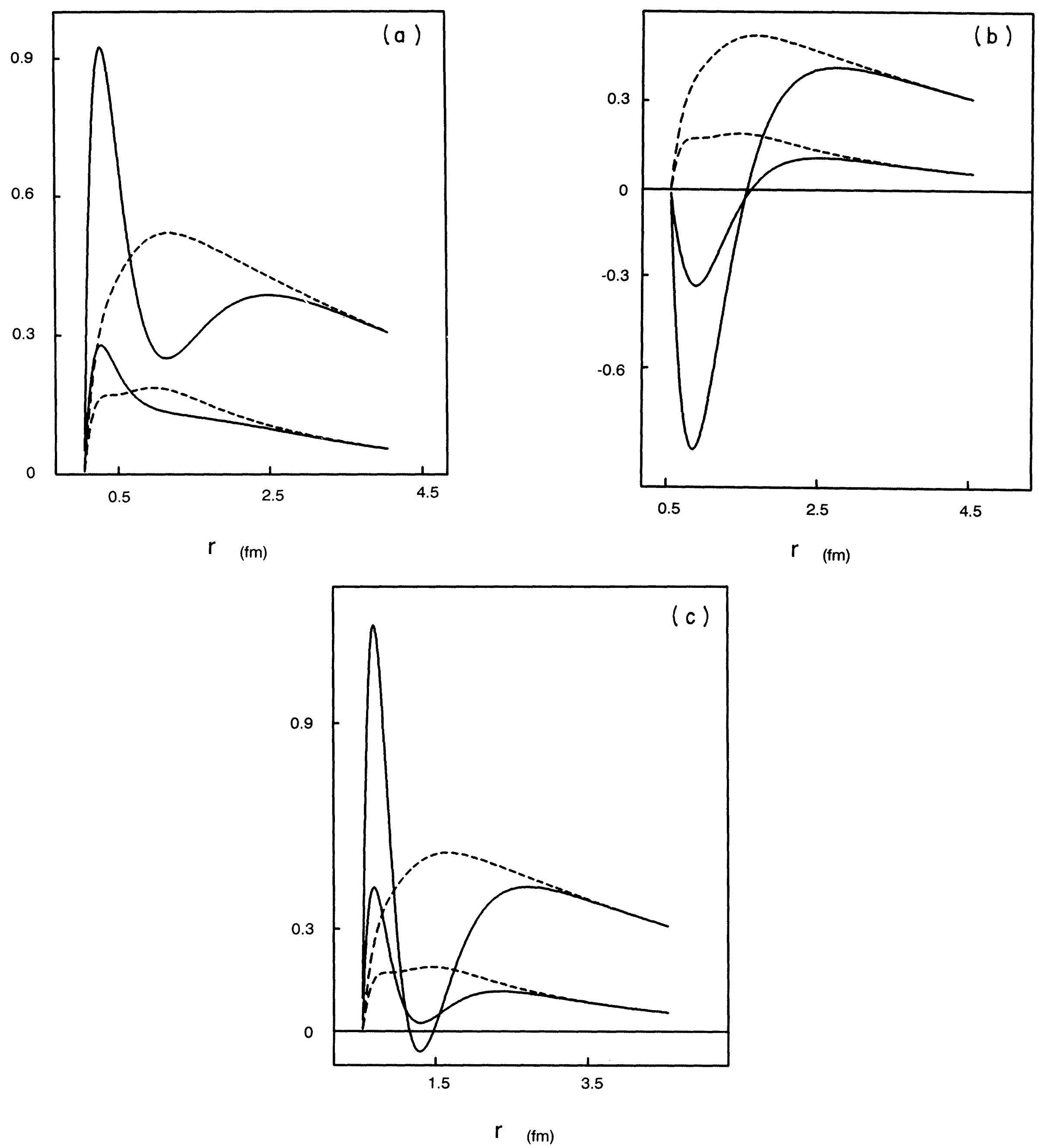

FIG. 7. The transformed radial deuteron wave functions with correct Q (solid lines) are compared to those of the reference local potential (dashed lines). Three pairs of values of α and β of Fig. 5(a) have been used: (a) $\alpha=3$ fm^{-1} and $\beta=1.633$ fm^{-1}, (b) $\alpha=3$ fm^{-1} and $\beta=-0.064$ fm^{-1}, and (c) $\alpha=4$ fm^{-1} and $\beta=2.436$ fm^{-1}. The upper (lower) curves are the u (w) wave functions.

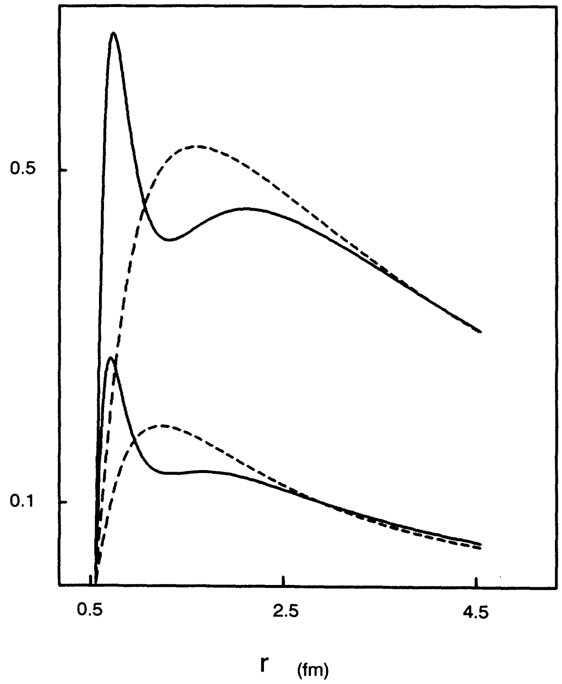

FIG. 8. The radial deuteron wave functions of the nonlocal potential of Table III (solid lines) are compared to those of the Reid hard-core (RHC) potential [25] (dashed lines). The upper (lower) curves are the u (w) wave functions.

where $\lambda = -325$ fm^{-3} is the nonlocality strength, $f(r) = e^{-\alpha r}$, and $\alpha = 2.1$ fm^{-1}.

During the computer search, the nonlocality strength parameter λ is fixed at a series of successively increasing negative values. For each of these values of λ, the potential free parameters A are adjusted in an attempt to fit the deuteron binding energy E_b, the quadrupole moment Q, the rms radius r_d, the triplet scattering length a_t, and the scattering parameter of Arndt *et al.* [31] in the laboratory scattering energy range 0–300 MeV. It was difficult to also fit the experimental value of the asymptotic S-state amplitude $A_S = 0.8838 \pm 0.0004$ fm$^{-1/2}$ [39] and the experimental value of the triplet effective range $r_t = 1.754 \pm 0.008$ fm [12] because of the correlations between r_d and A_S [11,41] and between r_d, a_t, and r_t [19,20]. The values of deuteron and low-energy scattering properties of this potential are given in Table IV. The radial deuteron wave functions of this nonlocal potential are compared to those of the Reid hard-core potential [25] in Fig. 8.

CONCLUSION

The two empirical linear ϵ_1-Q and η-$\gamma^2 Q$ relations, implied by the approximate relation of Blatt and Weisskopf [5], that have been found for standard nonrelativistic potential models of the deuteron are used to obtain two very similar values consistent with $Q^{\exp}$ for the deuteron asymptotic D/S ratio η. The criticality found in fitting Q, r_d, and a_t by a potential model points to a possible existence of a correlation between these quantities.

[1] R. V. Reid and L. M. Vaida, Phys. Rev. Lett. **29**, 494 (1972).
[2] D. M. Bishop and L. M. Cheung, Phys. Rev. A **20**, 381 (1979).
[3] M. H. MacGregor, R. A. Arndt, and R. H. Wright, Phys. Rev. **182**, 1714 (1969).
[4] P. Signell, Phys. Rev. C **2**, 1171 (1970).
[5] J. M. Blatt and V. F. Weisskopf, *Theoretical Nuclear Physics* (Wiley, New York, 1952), pp. 104–106, 112.
[6] L. C. Biedenharn and J. M. Blatt, Phys. Rev. **93**, 1387 (1954).
[7] M. N. Butler and D. W. L. Sprung, Can. J. Phys. **62**, 65 (1984).
[8] M. W. Kermode, J. R. Mines, and M. M. Mustafa, J. Phys. G **2**, L113 (1976).
[9] F. Tabakin, Ann. Phys. (N.Y.) **30**, 51 (1964).
[10] M. M. Mustafa, E. M. Zahran, and E. A. M. Sultan, J. Phys. G **18**, 303 (1992).
[11] S. Klarsfeld, J. Martorell, J. A. Oteo, M. Nishimura, and D. W. L. Sprung, Nucl. Phys. **A456**, 373 (1986).
[12] S. Klarsfeld, J. Martorell, and D. W. L. Sprung, J. Phys. G **10**, 165 (1984).
[13] M. M. Mustafa and E. M. Hassan, Phys. Scr. **39**, 522 (1989).
[14] W. van Dijk, Phys. Rev. C **40**, 1437 (1989).
[15] M. W. Kermode, S. A. Moszkowski, M. M. Mustafa, and W. van Dijk, Phys. Rev. C **43**, 416 (1991).
[16] M. W. Kermode, W. van Dijk, D. W. L. Sprung, M. M. Mustafa, and S. A. Moszkowski, J. Phys. G **17**, 105 (1991).
[17] M. M. Mustafa and M. W. Kermode, Few Body Systems **11**, 83 (1991).
[18] M. M. Mustafa, E. M. Hanssan, M. W. Kermode, and E. M. Zahran, Phys. Rev. C **45**, 2603 (1992).
[19] R. K. Bhaduri, W. Leidemann, G. Orlandini, and E. L. Tomusiak, Phys. Rev. C **42**, 1867 (1990).
[20] D. W. L. Sprung, H. Wu, and J. Martorell, Phys. Rev. C **42**, 863 (1990).
[21] A. McKerrell, M. W. Kermode, and M. M. Mustafa, J. Phys. G **3**, 1349 (1977).
[22] A. McKerrell, M. W. Kermode, J. R. Mines, and M. M. Mustafa, J. Phys. G **4**, 1349 (1977).
[23] M. Lacombe, B. Loiseau, J. M. Richard, R. Vinh Mau, J. Côté, P. Pirès, and R. de Tourreil, Phys. Rev. C **21**, 861 (1980).
[24] R. de Tourreil, B. Rouben, and D. W. L. Sprung, Nucl. Phys. **A242**, 445 (1975).
[25] R. V. Reid, Ann. Phys. (N.Y.) **50**, 411 (1968).
[26] T. Hamada and I. D. Johnston, Nucl. Phys. **34**, 382 (1962).
[27] N. K. Glendenning and G. Kramer, Phys. Rev. **126**, 2159 (1962).
[28] M. M. Mustafa and E. S. Zahran, Phys. Rev. C **38**, 2416 (1988).
[29] M. M. Mustafa (unpublished).
[30] C. Van der Leun and C. Alderliesten, Nucl. Phys. **A380**,

261 (1982).
[31] A. R. Arndt, L. D. Roper, R. A. Bryan, R. B. Clark, B. J. VerWest, and P. Signell, Phys. Rev. D **28**, 97 (1983).
[32] L. Mathelitsch and B. J. VerWest, Phys. Rev. C **29**, 739 (1984).
[33] H. P. Stapp, T. Ypsilantis, and N. Metropolis, Phys. Rev. **105**, 302 (1957).
[34] N. Hoshizaki, Prog. Theor. Phys. Suppl. **42**, 107 (1968).
[35] R. Machleidt, K. Holinde, and Ch. Elster, Phys. Rep. **149**, 1 (1987).
[36] R. Machleidt, Adv. Nucl. Phys. **19**, 189 (1989).
[37] M. M. Mustafa, Phys. Scr. **40**, 162 (1989).
[38] R. de Tourreil and D. W. L. Sprung, Nucl. Phys. **A201**, 193 (1973).
[39] V. G. J. Stoks, P. C. Van Campen, W. Spit, and J. J. de Swart, Phys. Rev. Lett. **60**, 1932 (1988).
[40] I. Borbély, W. Grüebler, B. Vuaridel, and V. König, Nucl. Phys. **A503**, 349 (1989).
[41] T. E. O. Ericson, Nucl. Phys. **A416**, 281c (1984).